FERMILAB-PUB-05-385-T
SLAC-PUB-11468
hep-ph/0509090

September 9, 2005

Comment on form factor shape and extraction of $|V_{ub}|$ from $B \to \pi l \nu$

Thomas Becher[(a)] and Richard J. Hill[(b)]

[(a)] *Fermi National Accelerator Laboratory,*
P. O. Box 500, Batavia, IL 60510, U.S.A.

[(b)] *Stanford Linear Accelerator Center, Stanford University*
Stanford, CA 94309, U.S.A.

Abstract

We point out that current experimental data for partial $B \to \pi l \nu$ branching fractions reduce the theoretical input required for a precise extraction of $|V_{ub}|$ to the form-factor normalization at a single value of the pion energy. Different parameterizations of the form factor shape leading to this conclusion are compared and the role of dispersive bounds on heavy-to-light form factors is clarified.

Submitted to Physics Letters B

Work supported in part by Department of Energy contract DE-AC02-76SF00515

1 Introduction

Measuring the magnitude of the weak mixing matrix element V_{ub} is important for constraining the unitarity triangle and testing the standard model of weak interactions. Inclusive and exclusive determinations from semileptonic B decays have different sources of experimental and theoretical systematic errors, and provide complementary determinations of this quantity.

Measurements of partial $B \to \pi l \nu$ branching fractions [1, 2, 3, 4] allow for a qualitatively distinct approach to extracting $|V_{ub}|$ compared to methods where only the total $B \to \pi l \nu$ branching fraction is available. Since the form factor shape is essentially fixed by experimental data, theoretical input is required only for a normalization of the relevant form factor. This normalization can be taken at an energy within the range currently studied with precision lattice simulations [5, 6]. In order to implement this program with reliable error estimates, three sources of uncertainty should be accounted for: first, experimental errors on the magnitudes of the partial branching fractions; second, theoretical errors for the form-factor normalization; and third, errors associated with incomplete knowledge of the form-factor shape used in fitting the combined data. While the first two sources are important (and the second of these is currently the dominant one), they do not pose obvious conceptual difficulties. The focus here is on the third source of error, and the extent to which the statement that the shape is "essentially fixed by experimental data" can be quantified.

Bounds on the form factor can be derived via the computation of an appropriately chosen correlation function in perturbative QCD. By analyticity, the resulting "dispersive bound" constrains the behavior of the form factor in the semileptonic region [7, 8, 9, 10], and may be expressed as a condition on the coefficients in a convergent expansion. This paper compares and relates the class of parameterizations emerging from the dispersive bound analysis to the class of parameterizations introduced in [11, 12]. Both classes are "exact" in the sense that the true form factor is guaranteed to be described arbitrarily well by a member of the class. We show that the determination of $|V_{ub}|$ is robust under the choice of parameterization and the number of parameters and discuss to what extent the same is true for form factor shape observables.

2 Form factor parameterizations and extraction of $|V_{ub}|$

Having restricted the shape of the q^2 spectrum, or equivalently, of the form factor, by experimental measurements, the central value and errors for $|V_{ub}|$ are determined by varying the allowed form factor over all "reasonable" curves that are consistent with the data, and with a normalization of the form factor taken from theory at a given value (or multiple values) of q^2. Defining this procedure precisely requires specifying a class of curves which contains the true form factor (to a precision compatible with the data), and which is sufficiently rich to describe all variations that impact the observables under study. A statistical analysis along standard lines then determines central values and errors for the desired observable quantities.

A starting point for isolating such a class of curves is the dispersive representation of the

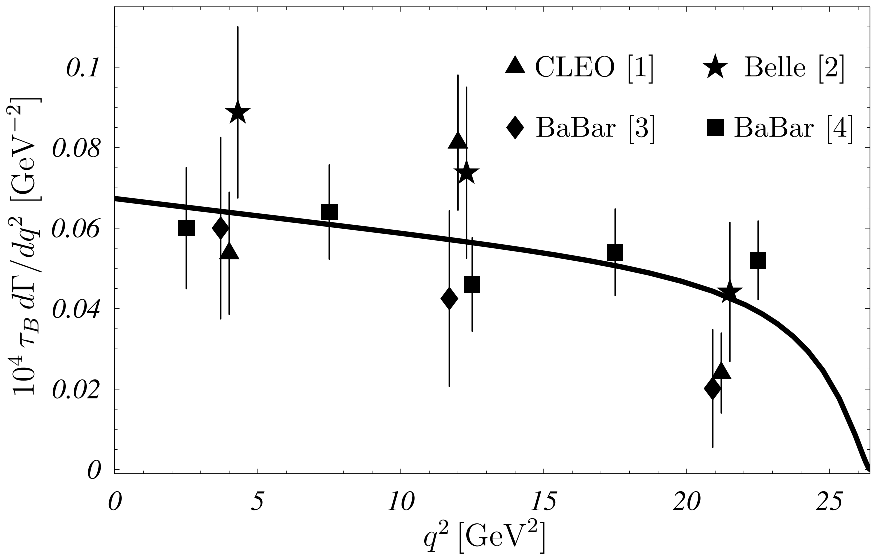

Figure 1: Experimental data for the partial $\bar{B}^0 \to \pi^+\ell^-\bar{\nu}$ branching ratios and fit result shown as solid line. The fit results from (2) with $N = 1$ and (5) with $k_{\rm max} = 2$ are indistinguishable. Note that the experimental data is binned: [1, 2, 3] give the result in three bins, while [4] gives the result in five q^2-bins. We plot the value and error divided by the bin width at the average q^2-value in each bin. For the three-bin results, we have slightly shifted the points to the left and right to increase visibility.

relevant form factor:

$$F_+(q^2) = \frac{F_+(0)/(1-\alpha)}{1 - \frac{q^2}{m_{B^*}^2}} + \frac{1}{\pi}\int_{t_+}^{\infty} dt\,\frac{{\rm Im}F_+(t)}{t - q^2 - i\epsilon}\,. \tag{1}$$

Here α is defined by the relative size of the contribution to $F_+(0)$ from the B^* pole, and $t_\pm \equiv (m_B \pm m_\pi)^2$. For massless leptons, the semileptonic region is given by $0 \le q^2 \le t_-$. Equation (1) states that, after removing the contribution of the B^* pole lying below threshold, $F_+(q^2)$ is analytic outside of a cut in the complex q^2-plane extending along the real axis from t_+ to ∞, corresponding to the production region for states with the appropriate quantum numbers.

One class of parameterizations keeps the B^* pole explicit and approximates the remaining dispersion integral in (1) by a number of effective poles:

$$F_+(q^2) = \frac{F_+(0)/(1-\alpha)}{1 - \frac{q^2}{m_{B^*}^2}} + \sum_{k=1}^{N} \frac{\rho_k}{1 - \frac{1}{\gamma_k}\frac{q^2}{m_{B^*}^2}}\,. \tag{2}$$

The true form factor can be approximated to any desired accuracy by introducing arbitrarily many, finely-spaced, effective poles. In the next section, we derive a bound on the magnitudes of the coefficients of the effective poles, $|\rho_k|$. This allows a meaningful $N \to \infty$ limit, thus enabling us to investigate the behavior of the fits when arbitrarily many parameters are included.

We find that current data cannot yet resolve more than one distinct effective pole in addition to the B^* pole. Parameterizations of the above type are widely used to fit form factors. In particular, a simplified version of the $N = 1$ case, the so-called Becirevic-Kaidalov (BK) parameterization [11] is used in many recent lattice calculations and experimental studies. As shown in [12], this two-parameter form is overly restrictive since it enforces scaling relations which at small q^2 are broken by hard gluon exchange. The size of these hard-scattering terms, which appear at leading order in the heavy-quark expansion, is subject to some controversy and constraining their size is an important task. The parameterization of the form factors should allow for their presence.

Another class of parameterizations is obtained by expanding the form factor in a series around some $q^2 = t_0$ in the semileptonic region up to a fixed order, with the coefficients of this expansion as the fit parameters. However, the convergence of this simple expansion in the semileptonic region is very poor due to the presence of the nearby singularities at $q^2 = m_{B^*}^2$ and $q^2 = t_+$. An improved series expansion of the form factor that converges in the entire cut q^2-plane is obtained after a change of variables that maps this region onto the unit disc $|z| < 1$. In terms of the new variable, F_+ has an expansion

$$F_+(q^2) = \frac{1}{P(q^2)\phi(q^2,t_0)} \sum_{k=0}^{\infty} a_k(t_0)\,[z(q^2,t_0)]^k\,, \quad z(q^2,t_0) = \frac{\sqrt{t_+ - q^2} - \sqrt{t_+ - t_0}}{\sqrt{t_+ - q^2} + \sqrt{t_+ - t_0}}\,, \tag{3}$$

with real coefficients a_k. The variable $z(q^2, t_0)$ maps the interval $-\infty < q^2 < t_+$ onto the line segment $-1 < z < 1$, with the free parameter $t_0 \in (-\infty, t_+)$ corresponding to the value of q^2 mapping onto $z = 0$. Points immediately above (below) the q^2-cut are mapped onto the lower (upper) half-circle $|z| = 1$. The function $P(q^2) \equiv z(q^2, m_{B^*}^2)$ accounts for the pole in $F_+(q^2)$ at $q^2 = m_{B^*}^2$, while $\phi(q^2)$ is any function analytic outside of the cut. It is interesting to note that this reorganization succeeds in turning a large recoil parameter, $(v \cdot v')_{\max} - 1 \approx 18$, into a small expansion parameter. For example, for $t_0 = 0$ the variable z is negative throughout the semileptonic region and

$$|z|_{\max} = \frac{\sqrt{(v\cdot v')_{\max} + 1} - \sqrt{2}}{\sqrt{(v\cdot v')_{\max} + 1} + \sqrt{2}} \approx 0.5\,, \tag{4}$$

where v and v' are the velocities of the B and π mesons. The same size, but for positive z is obtained for $t_0 = t_-$. By choosing the intermediate value $t_0 = t_+(1 - \sqrt{1 - t_-/t_+})$, the expansion parameter can be made as small as $|z|_{\max} \approx 0.3$. A second class of parameterizations is obtained by a truncation of the above series:

$$F_+(q^2) = \frac{1}{P(q^2)\phi(q^2,t_0)} \sum_{k=0}^{k_{\max}} a_k(t_0)\,[z(q^2,t_0)]^k\,. \tag{5}$$

As discussed in the next section, it is conventional to take

$$\phi(q^2,t_0) = \left(\frac{\pi m_b^2}{3}\right)^{1/2} \left(\frac{z(q^2,0)}{-q^2}\right)^{5/2} \left(\frac{z(q^2,t_0)}{t_0 - q^2}\right)^{-1/2} \left(\frac{z(q^2,t_-)}{t_- - q^2}\right)^{-3/4} \frac{(t_+ - q^2)}{(t_+ - t_0)^{1/4}}\,. \tag{6}$$

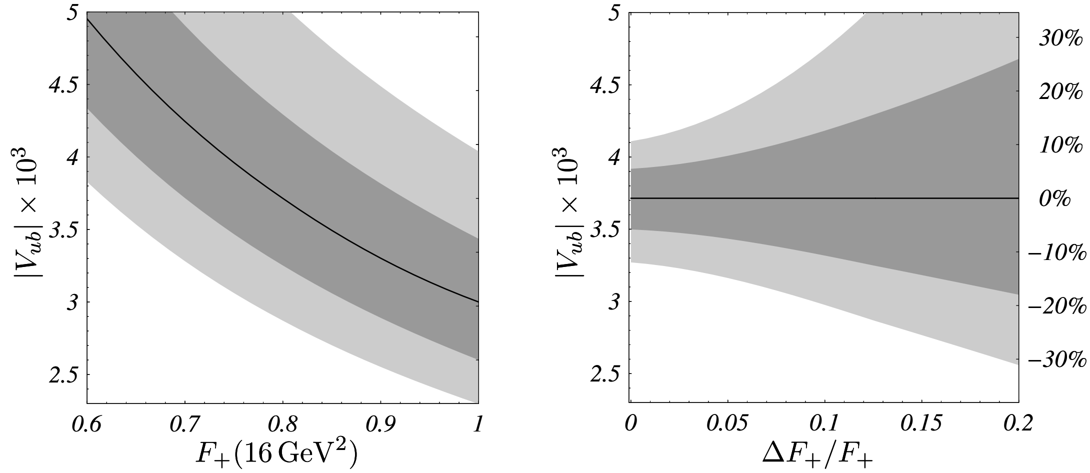

Figure 2: 68% (dark) and 95% (light) confidence limits for $|V_{ub}|$ determined by fitting the parameterizations (2) or (5) to experimental data in [1], [2], [3] and [4], with the single lattice data point $F_+(16\,\mathrm{GeV}^2) = 0.8 \pm 0.1$. Results from (2) and (5) are indistinguishable. The plot on the right shows $|V_{ub}|$ for fixed $F_+(16\,\mathrm{GeV}^2) = 0.8$ as a function of the relative uncertainty on the form-factor.

With this choice, a bound $\sum_k a_k^2 \lesssim 1$ is obtained by perturbative methods. [1] Together with the restriction $|z| < 1$, this allows a meaningful $k_{\max} \to \infty$ limit. We find that current data can only resolve the first three terms in the series (5).

Figure 1 shows the available experimental data on the partial branching fraction $d\Gamma(\bar{B}^0 \to \pi^+\ell^-\bar{\nu})/dq^2$. The CLEO [1], Belle [2] and BaBar [4] collaborations have measured this branching fraction in three separate q^2-bins and BaBar [3] has presented a measurement using five q^2-bins. In order to extract $|V_{ub}|$ we also need the normalization of the form factor $F_+(q^2)$. The $B \to \pi$ vector form factors have recently been determined by the Fermilab Lattice [5] and by the HPQCD [6] collaborations in lattice simulations with dynamical fermions. The preliminary results of these calculations give $F_+(16\,\mathrm{GeV}^2) = 0.81 \pm 0.11$ [5] and $F_+(16\,\mathrm{GeV}^2) = 0.73 \pm 0.10$ [6]. [2] The lattice calculations give the form factor at several different q^2-values. However, the correlations between different points are not available and it

[1]For different t_0, the expansion parameters, $z \equiv z(t,t_0)$ and $z' \equiv z(t,t_0')$, and expansion coefficients, $a_k \equiv a_k(t_0)$ and $a_k' \equiv a_k(t_0')$, are related by the Möbius transformation:

$$z' = \frac{z(t_0,t_0') + z}{1 + z(t_0,t_0')z}\,, \qquad \sqrt{1-z^2}\sum_{k=0}^{\infty} a_k z^k = \sqrt{1-z'^2}\sum_{k=0}^{\infty} a_k' z'^k\,.$$

It is easily verified that the sum of squares of coefficients is invariant under such a transformation, $\sum_k a_k^2 = \sum_k {a_k'}^2$, as guaranteed by the construction of ϕ, see (9).

[2]The parameterization (2) with $N = 1$ has been used to interpolate to the common q^2-point, and for definiteness the errors are taken as those from the nearest points: $q^2 = 15.87\,\mathrm{GeV}^2$ [5], with statistical and systematic errors added in quadrature, and $q^2 = 16.28\,\mathrm{GeV}^2$ [6].

is difficult to quantify the uncertainty on the shape. Here, we do not use any shape information from the lattice, and use $F_+(16\,\mathrm{GeV}^2) = 0.8 \pm 0.1$ as our default value for the form factor normalization. Performing a χ^2 fit yields $|V_{ub}| = 3.7^{+0.6}_{-0.5} \times 10^{-3}$ for both the parameterization (2) with $N = 1$, and (5) with $k_{\max} = 2$. The correlation matrix is included for the data in [1]. For the remaining data, q^2-bins are taken as uncorrelated.

Figure 2 shows the 68% and 95% confidence limits for $|V_{ub}|$ as a function of the value and uncertainty of the form factor at $q^2 = 16\,\mathrm{GeV}^2$. The form factor normalization is the dominant error in the determination of $|V_{ub}|$; if the quantity $F_+(16\,\mathrm{GeV}^2)$ would be known exactly, the uncertainty on $|V_{ub}|$ would drop to approximately 6%. The quality of the fit is equally good for both parameterizations, with $\chi^2 = 12.0$. [3] The extracted value of $|V_{ub}|$ is insensitive to the choice of the free parameter t_0. Setting $\phi(q^2) = 1$ in (5) also has negligible impact, and similarly adding more lattice input points does not substantially change the result if the dominant lattice errors are correlated. The effect of allowing additional terms in the parameterizations (2) and (5) is investigated in the following sections. We will find that the result for the value and uncertainty of $|V_{ub}|$ from the simple parameterizations used in this section is not appreciably altered if additional terms are included in the parameterizations of the form factor.

3 Form factor bounds

To make a fully rigorous determination of $|V_{ub}|$, the truncation to the three-parameter classes of curves considered in the previous section requires justification. For instance, if the neglected terms in (2) or (5) conspired to produce a sharp peak in the form factor at precisely the value of the lattice input point, then the integrated rate would be overestimated, and the value of $|V_{ub}|$ underestimated. To prevent this from happening requires some bound on the perversity of allowed form-factor shapes.

To bound the coefficients ρ_k in the expansion (2), we introduce a decomposition of the integration region, $t_+ \le t_1 < \cdots < t_{N+1} < \infty$, and define

$$\rho_k \equiv \frac{1}{\pi} \int_{t_k}^{t_{k+1}} \frac{dt}{t} \, \mathrm{Im} F_+(t) \,, \quad \gamma_k \equiv \frac{t_k}{m_{B^*}^2} \,. \tag{7}$$

Since $F_+(t) \sim t^{-1}$ at large t, it follows that

$$\sum_k |\rho_k| \le \frac{1}{\pi} \int_{t_+}^{\infty} \frac{dt}{t} |F_+(t)| \equiv R \,, \tag{8}$$

and this is the desired bound. Assuming the integral in (8) is dominated by states with $t - t_+ \sim m_b \Lambda$, where $F_+ \sim m_b^{1/2}$, the quantity R is parametrically of order $(\Lambda/m_b)^{1/2}$, with

[3] Note that all three-bin measurements determine the same observable quantities. The minimal χ^2 obtained from the three-bin measurements is 5.0 for $9-3$ degrees of freedom. This value measures the (good) agreement between the three-bin measurements, and should be subtracted from the total in order to obtain a measure of agreement between the data and the parameterizations. The resulting quality of our fit is good: $12.0 - 5.0$ for $9 - 4$ degrees of freedom.

Λ a hadronic scale. To be sure that the bound deserves the model-independent moniker, one should use a very conservative estimate. In our fits we will use $R = \sqrt{10}$ and $R = 10$.

The coefficients a_k in the expansion (5) can be bounded by requiring that the production rate of $B\pi$ states, described by the analytically continued form factor, does not overwhelm the production rate of *all* states coupling to the current of interest (in this case, the vector current $\bar{u}\gamma^\mu b$). The latter rate is computable in perturbative QCD using the operator product expansion (see e.g. [10]). The function ϕ in (6) was chosen such that the fractional contribution of $B\pi$ states to this rate is given at leading order by

$$\sum_{k=0}^{\infty} a_k^2 = \frac{1}{2\pi i}\oint \frac{dz}{z}|\phi(z)P(z)F_+(z)|^2 = \frac{m_b^2}{3}\int_{t_+}^{\infty}\frac{dt}{t^5}[(t-t_+)(t-t_-)]^{3/2}|F_+(t)|^2 < 1\,. \tag{9}$$

Assuming that the integral in (9) is dominated by states with $t - t_+ \sim m_b\Lambda$, where $F_+ \sim m_b^{1/2}$, the bounded quantity is parametrically of order $(\Lambda/m_b)^3$. Since, by definition, the fraction is smaller than unity, it is conventional to take the loose bound $\sum_{k=0}^{\rm k_{max}} a_k^2 < 1$, which does not make use of scaling behavior in the heavy-quark limit. Clearly this bound leaves much room for improvement; from its scaling behavior, we expect $\sum_{k=0}^{\infty} a_k^2$ to be of the order of a few permille. This implies that higher-order perturbative and power corrections in the operator product analysis introduce negligible error, as noticed in [13]. It is also easy to see that the dispersive bounds by themselves do not impose tight constraints on the form factor shape. Since the scale of the coefficients is set by $a_0 \sim m_b^{-3/2}$, even with the optimal choice $|z|_{\rm max} \approx 0.3$, the dispersive bounds allow the relative size of higher-order terms in the series, $|a_k z^k/a_0|$, to be of order unity up to $k \approx 4$, and to contribute significantly for even higher k. This situation for heavy-to-light decays such as $B \to \pi$ contrasts with that for heavy-heavy decays such as $B \to D$ [14, 15], where the bound is parametrically of order unity (counting $m_c \sim m_b \gg \Lambda$). For this case, the scale of the coefficients is set by $a_0 \sim m_b^0$, and with $|z|_{\rm max} \approx 0.06$ the bound ensures that only the first few terms in the series are required for percent accuracy.

To put the dispersive bounds in perspective, it may be useful to emphasize that establishing an order-of-magnitude bound on any integral of the form $\int_{t_+}^{\infty} dt\, k(t)|F_+(t)|^2$ for some $k(t)$ would yield an equally valid, bounded, parameterization, with a new $\phi(t)$ constructed from $k(t)$ as in (6) and (9). Similarly, bounded pole parameterizations (2) are obtained by establishing an order-of-magnitude bound on any integral of the form $\int_{t_+}^{\infty} dt\, k(t)|F_+(t)|$ for some $k(t)$, as in (7) and (8). Focusing attention on the special case of (6) and (9) is justified only to the extent that the bound (9) is sufficiently restrictive, and to the extent that similar or tighter bounds cannot be conservatively estimated by other means.

It is interesting to note that the two bounds are not equivalent. The bound $\sum_k |\rho_k| < R$ uses the fact that the asymptotic form factor can be evaluated in perturbation theory, where the scaling $F_+(t) \sim t^{-1}$ is found at large t. This condition is not automatically satisfied by the series parameterization (5), which as seen from (9) requires only $F_+(t) \lesssim t^{1/2}$ at large t. Imposing the proper large-t behavior yields the sum rules

$$\frac{d^n}{dz^n}P(z)\phi(z)F(z)\bigg|_{z=1} = 0 \quad \leftrightarrow \quad \sum_{k=0}^{\infty} k^n\, a_k z^k\bigg|_{z\to 1} = 0\,, \quad n = 0, 1, 2. \tag{10}$$

To our knowledge, the above sum rules have not been discussed in the literature. On the other hand, all pole parameterizations "violate" the bound $\sum_{k=0}^{\infty} a_k^2 < 1$ for the simple reason that the integral in (9) is not well defined for these parameterizations, because $F_+(t)$ has poles on the integration contour.

The bounds discussed here are associated with the behavior of the form factor above threshold. Since we are interested in the form factor in the semileptonic region, these higher-energy properties are useful only to the extent that they can help to constrain the form factor in this region. Incorrect high-energy behavior therefore does not imply that a given parameterization cannot be used to parameterize low-energy data. For instance, the effective poles in (2) could be smeared into finite-width effective resonances in order to make the integral in (9) converge; however, the semileptonic data is very insensitive to such fine-grained detail, and this modification has a very minor impact on the fits. Similarly, unless the bound (9) is close to being saturated, the coefficients a_k for moderately large k in the series parameterization (5) can be tuned to satisfy the sum rules (10), or equivalently, to make the integral in (8) converge. However, the semileptonic data becomes insensitive to terms z^k for large k, and again such a modification has little impact on the fits. Thus, while at some level the bound (8) will constrain the parameters in the series parameterization (5), and the bound (9) will constrain the parameters in the pole parameterization (2), we restrict attention to the constraints imposed by (8) on the pole parameterization, and by (9) on the series parameterization.

4 Parameterization uncertainty and shape observables

Imposing the bound $\sum_k |\rho_k| < 10$, we observe that additional poles in the class of parameterizations (2) have essentially no impact on the central value and errors for $|V_{ub}|$. Similarly, using the bound $\sum_k a_k^2 < 1$ in (5) we find that the inclusion of higher order terms beyond $k_{\max} = 2$ has negligible impact on $|V_{ub}|$. The errors are dominated by the lattice input point, and both the central value and errors are not changed significantly from the $N = 1$ or $k_{\max} = 2$ fits in the previous section.

In order to isolate the uncertainty on the form factor shape inherent to the data, we show in Figure 3 the minimum attainable error on $|V_{ub}|$ with present data, assuming exact knowledge of the form factor at one q^2-value. Results are shown for the parameterization (5), using various bounds $\sum_k a_k^2 < 0.01$, 0.1 and 1. As the figure illustrates, points in the intermediate range of q^2 lead to the smallest uncertainty on $|V_{ub}|$, and for these points, the $|V_{ub}|$ extraction is not very sensitive to even the order of magnitude of the chosen bound, with the minimum error varying from approximately 6% to approximately 8% as the bound is relaxed from 0.01 to 1. It should be noted that a better understanding of correlations in the experimental data would be necessary when probling this level of precision. The curves in Figure 3 are also indicative of the impact of additional theory inputs. Performing the fits with data points at different q^2-values in addition to the default $F_+(16\,\mathrm{GeV}^2)$ shows that a point at $q^2 = 0$ would require $\lesssim 10\%$ error to significantly decrease the error on $|V_{ub}|$, while even exact knowledge of the form factor at $q^2 = t_-$ has almost no impact.

In the remainder of this section we consider observables which are more sensitive to the shape of the form factor and investigate the role played by the bounds in these cases. In par-

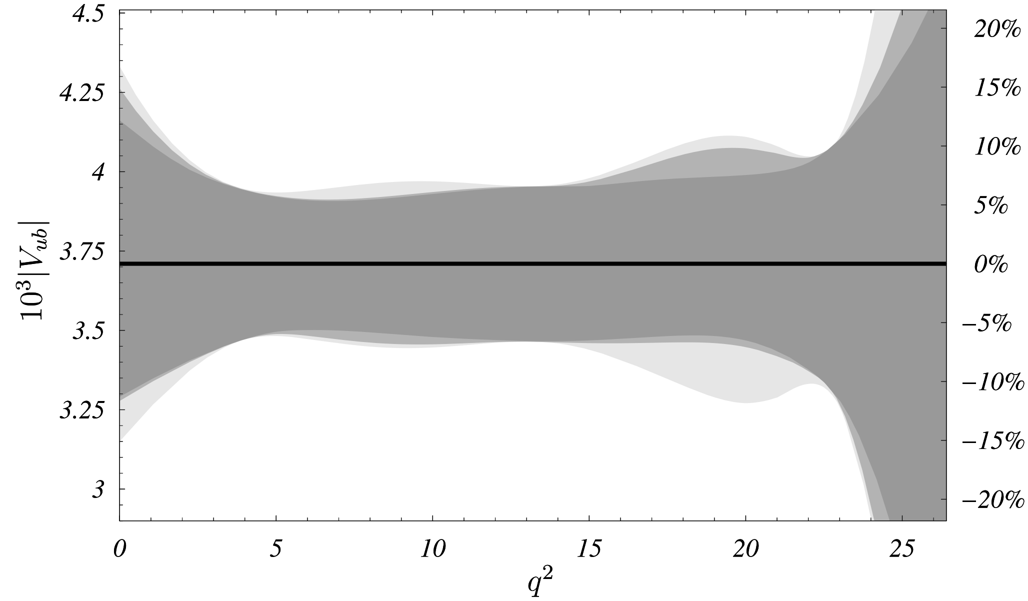

Figure 3: $\Delta\chi^2 = 1$ region for $|V_{ub}|$ for an infinitely precise form-factor determination at a single q^2-value. The plot assumes that the form factor yields the central value $|V_{ub}| = 3.7 \times 10^{-3}$. The darkest band is obtained for $\sum_k a_k^2 < 0.01$, while the two lighter bands correspond to $\sum_k a_k^2 < 0.1$ and $\sum_k a_k^2 < 1$.

ticular, we extract the form factor and its first derivative at $q^2 = 0$, as well as the residue at the B^* pole, which is directly related to the parameter α, as in (1). These quantities are interesting in their own right. The form factor at zero momentum transfer, normalized as $|V_{ub}|F_+(0)$, is an important input for the evaluation of factorization theorems for charmless two-body decays such as $B \to \pi\pi$. The derivative of the form factor at $q^2 = 0$, conveniently normalized as $(m_B^2 - m_\pi^2)F'_+(0)/F_+(0)$, determines the quantity δ measuring the ratio of hard-scattering to soft-overlap terms in the form factor [12]. Finally, the value of $(1-\alpha)^{-1}$ is proportional to the coupling constant $g_{B^*B\pi}$. The observable quantities $|V_{ub}|F_+(0)$, $F'_+(0)/F_+(0)$ and α are independent of the form-factor normalization, and hence are determined solely by the experimental data.

In Tables 1 and 2, we show how the results for the shape observables change when additional parameters are added into the fit. For the pole parameterization (2) we perform fits with $N = 1$, 2 and 3 poles in addition to the B^* pole. (The case $N = 1$ was studied in [12].) To help stabilize the fits, we impose a minimum spacing of the poles $\gamma_{k+1} - \gamma_k > 1/N$, and a maximum pole position, $\gamma_k < N + 1$. For the polynomial parameterization (5), we set $k_{\max} = 2$, 3 and 4. We perform each of the fits with two different bounds — a loose model-independent bound, and a more stringent bound that relies on the scaling behavior of the bounded quantity in the heavy-quark limit. Given a value of the bound, a central value and errors are determined by taking the limit of large N in (2), or large $k_{\max}$ in (5). The sequence converges once the size of the neglected terms is constrained by the bound to lie below the

bound	$\sum_k \lvert\rho_k\rvert = 10$			$\sum_k \lvert\rho_k\rvert = \sqrt{10}$		
N	1	2	3	1	2	3
$\sum_k \lvert\rho_k\rvert$	1.02	1.36	10	1.02	1.36	$\sqrt{10}$
χ^2	11.97	11.96	11.58	11.97	11.96	11.80
$10^3\lvert V_{ub}\rvert F_+(0)$	$0.93^{+0.06}_{-0.09}$	$0.93^{+0.11}_{-0.09}$	$0.87^{+0.14}_{-0.12}$	$0.93^{+0.06}_{-0.09}$	$0.93^{+0.10}_{-0.09}$	$0.91^{+0.11}_{-0.10}$
$\frac{(m_B^2-m_\pi^2)F'_+(0)}{F_+(0)}$	$1.3^{+0.4}_{-0.1}$	$1.3^{+0.4}_{-0.7}$	$2.0^{+0.9}_{-1.2}$	$1.3^{+0.4}_{-0.1}$	$1.3^{+0.4}_{-0.6}$	$1.5^{+0.6}_{-0.8}$
$(1-\alpha)^{-1}$	5^{+5}_{-3}	6^{+6}_{-5}	6^{+20}_{-15}	5^{+5}_{-3}	6^{+6}_{-5}	6^{+6}_{-8}

Table 1: Fit results for form factor shape parameters using the pole parameterization (2).

sensitivity of the chosen observable.

The quantities $|V_{ub}|F_+(0)$, $F'_+(0)/F_+(0)$ and α exhibit different sensitivities to the bounds. This is to be expected, since sharp bends in the fitted curve at the endpoints allowed by the additional terms can have strong effects on the slope, or on the residue of the B^* pole, but are not constrained tightly by the data. Imposing only very loose bounds therefore leads to large uncertainties for these quantities.

It is instructive to examine the relation between observables and expansion coefficients. At $t_0 = 0$ the quantities $f(0)$, α, β and δ in [12] are related to the coefficients a_k by

$$
\begin{aligned}
f(0) \equiv F_+(0) &= \frac{16a_0}{\hat{m}_b}\left(\frac{3}{\pi}\right)^{1/2}\frac{(1+\hat{m}_\pi)^{5/2}}{(1+\sqrt{\hat{m}_\pi})^3}\frac{1+\hat{m}_\pi+\hat{\Delta}}{1+\hat{m}_\pi-\hat{\Delta}}\,, \\
1+\beta^{-1}-\delta \equiv \frac{m_B^2-m_\pi^2}{F_+(0)}\left.\frac{dF_+}{dq^2}\right|_{q^2=0} &= \frac{-a_1}{4a_0}\frac{1-\hat{m}_\pi}{1+\hat{m}_\pi}+\frac{3}{4}\frac{1-\sqrt{\hat{m}_\pi}}{1+\sqrt{\hat{m}_\pi}}+\frac{\hat{\Delta}(1-\hat{m}_\pi)}{(1+\hat{m}_\pi)^2-\hat{\Delta}^2}\,, \\
(1-\alpha)^{-1} &= \frac{(1+\hat{m}_\pi+\hat{\Delta})^2(1+\sqrt{\hat{m}_\pi})^3}{4(1+\hat{m}_\pi)^2(\hat{\Delta}+2\sqrt{\hat{m}_\pi})^{3/2}}\sum_{k=0}^{\infty}\frac{a_k}{a_0}\left((-1)\frac{1+\hat{m}_\pi-\hat{\Delta}}{1+\hat{m}_\pi+\hat{\Delta}}\right)^k\,,
\end{aligned}
\tag{11}
$$

where $\Delta^2 \equiv (m_B+m_\pi)^2 - m_{B^*}^2$, and hats denote quantities in units of m_B. From the heavy-quark scaling laws for the quantities appearing on the left-hand side, it follows that $a_0 \sim m_b^{-3/2}$, $a_1 \sim m_b^{-3/2}$, and that the sum in the last line scales as $\hat{\Delta}^{-1/2} \sim m_b^{1/4}$.

5 Results and discussion

In order to extract the most precise value of $|V_{ub}|$, it is important to make full use of the existing experimental data for $B \to \pi l \nu$ that determines the form factor shape. To emphasize this point, the analysis was done here using no shape information at all from theory, but only a normalization at one q^2-point. Our results make it clear that the limiting factor in the determination of $|V_{ub}|$ is currently the form factor normalization, with very small uncertainty

bound	$\sum_k a_k^2 < 1$			$\sum_k a_k^2 < 0.01$		
$k_{\max}$	2	3	4	2	3	4
$\sum a_k^2$	0.003	0.3	1	0.003	0.01	0.01
χ^2	12.0	11.7	11.7	12.0	11.9	11.9
$10^3 \lvert V_{ub}\rvert F_+(0)$	$0.93^{+0.10}_{-0.10}$	$0.87^{+0.15}_{-0.15}$	$0.87^{+0.14}_{-0.14}$	$0.93^{+0.10}_{-0.10}$	$0.92^{+0.11}_{-0.10}$	$0.92^{+0.11}_{-0.10}$
$\frac{(m_B^2-m_\pi^2)F_+'(0)}{F_+(0)}$	$1.3^{+0.6}_{-0.5}$	$2.0^{+1.4}_{-1.4}$	$2.0^{+1.4}_{-1.4}$	$1.3^{+0.6}_{-0.4}$	$1.4^{+0.6}_{-0.6}$	$1.5^{+0.6}_{-0.6}$
$(1-\alpha)^{-1}$	6^{+2}_{-2}	13^{+8}_{-14}	9^{+20}_{-17}	6^{+2}_{-2}	7^{+2}_{-5}	8^{+2}_{-6}

Table 2: Fit results for form factor shape parameters using the series parameterization (5) with $t_0 = 0$.

associated with the form factor shape. Similar conclusions are implicit in other recent works. For example, in [13] the reduction in error compared to methods employing only total experimental branching fractions is due almost entirely to the inclusion of shape information from experiment, and not to the inclusion of additional theory input points, or to the use of dispersive bounds. In [16], shape information from experiment is used to constrain the hadronic input parameters appearing in sum rule estimates of the form factor.

In practical terms, the parameterizations (2), with $N = 1$, and (5), with $k_{\max} = 2$, are sufficient for describing the current generation of semileptonic data, in the sense that the addition of more parameters does not significantly improve the fits. For "global" quantities like $|V_{ub}|$ it is possible to show by imposing only the loose bounds $\sum_k |\rho_k| < 10$ in (2), or $\sum_k a_k^2 < 1$ in (5) that the extracted values are insensitive to the addition of more parameters. With a single lattice input value $F_+(16\,\mathrm{GeV}^2) = 0.8 \pm 0.1$,

$$\begin{aligned} |V_{ub}| &= 3.7 \pm 0.2\,^{+0.6}_{-0.4} \pm 0.1 &&= (3.7 \pm 0.2) \times \frac{0.8}{F_+(16\,\mathrm{GeV}^2)}\,, \\ F_+(0) &= 0.25 \pm 0.04 \pm 0.03 \pm 0.01 &&= (0.25 \pm 0.04) \times \frac{F_+(16\,\mathrm{GeV}^2)}{0.8}\,. \end{aligned} \tag{12}$$

The first error is experimental, the second is theoretical from the lattice input, and the third is due to the uncertainty in the form factor shape. For definiteness, the central values in (12) are obtained using the parameterization (5) with $\sum_k a_k^2 < 0.01$, and the third error is very conservatively estimated by adding the maximum variation of the boundaries of the 1σ interval induced by relaxing the bound to $\sum_k a_k^2 < 1$.

For less global quantities, like the slope of the form factor at $q^2 = 0$, the bound (9) is not sufficient to tightly constrain the impact of arbitrarily many additional parameters. In this case we find

$$\begin{aligned} 10^3 |V_{ub} F_+(0)| &= 0.92 \pm 0.11 \pm 0.03\,, \\ (m_B^2 - m_\pi^2)\frac{F_+'(0)}{F_+(0)} &= 1.5 \pm 0.6 \pm 0.4\,, \end{aligned} \tag{13}$$

$$(1-\alpha)^{-1} = 8\,^{+2}_{-7} \pm 7\,.$$

The first error is experimental, and the second is due to uncertainty in the form factor shape (these quantities are independent of the form factor normalization). The latter error is estimated by adding the maximum variation of the boundaries of the 1σ interval when the bound is relaxed to $\sum_k a_k^2 < 0.1$.

While the dispersive bound approach provides an elegant means of demonstrating formal convergence properties with the minimal assumption of form-factor analyticity and the convergence of an operator product expansion, some caution is required in order to avoid misinterpreting the results. Firstly, for certain observables, e.g. $|V_{ub}|$, the fits are much more tightly constrained by the data than by the dispersive bounds. This leads to the happy conclusion that the errors on $|V_{ub}|$ do not depend on the chosen parameterization or the exact value of the bound, and the analysis lends itself to a straightforward statistical interpretation. Secondly, other important observables, such as the slope of the form factor, *are* sensitive to the addition of more parameters than can be constrained by the data, but are allowed by the dispersive bound. Since this bound is overestimated, presumably by orders of magnitude, a reliance on this procedure would lead to the pessimistic conclusion that almost no information at all can be extracted from the data for these quantities. In such cases, we propose to use tighter bounds, which follow from the scaling behavior of the bounded quantity in the heavy quark limit.

Apart from establishing order-of-magnitude estimates for the bounds in (8) and (9) by heavy-quark power counting, none of the above analysis relies on heavy-quark, large-recoil or chiral expansions, or on the associated heavy-quark, soft-collinear or chiral effective field theories. However, the semileptonic data can be used to test predictions from these effective field theories, and to determine low-energy parameters that can be used as inputs to the calculation of other processes. For example, using the experimental result $\mathrm{Br}(B^- \to \pi^-\pi^0) = (5.5 \pm 0.6) \times 10^{-6}$ [17] together with $|V_{ub}|F_+(0)$ from (13), we find

$$\frac{\Gamma(B^- \to \pi^-\pi^0)}{d\Gamma(\bar{B}^0 \to \pi^+\ell^-\bar{\nu})/dq^2|_{q^2=0}} = 0.76\,^{+0.22}_{-0.18} \pm 0.05\,\mathrm{GeV}^2\,, \tag{14}$$

where the first error is experimental, and the second is due to the form-factor shape uncertainty in (13). Such ratios provide a strong test of factorization [18]. The leading-order prediction for this ratio, corresponding to the "naive" factorization picture where hard-scattering terms are neglected, yields $16\pi^2 f_\pi^2 |V_{ud}|^2 (C_1 + C_2)^2/3 = 0.62 \pm 0.07\,\mathrm{GeV}^2$. The uncertainty includes only the effects of varying the renormalization scale of the leading-order weak-interaction coefficients [19] between $m_b/2$ and $2m_b$. This may be compared to the prediction of Beneke and Neubert [20] who use QCD factorization theorems for two-body decays to work beyond leading order and include the effects of hard-scattering terms, obtaining for the same ratio, $0.66\,^{+0.13}_{-0.08}\,\mathrm{GeV}^2$. The uncertainty in their prediction is dominated by the uncertainty in the light-cone distribution amplitudes (LCDAs) of the B- and π-mesons. Bauer et al. [21, 13] evaluate the same factorization theorems using a different strategy: they use experimental results for other $B \to \pi\pi$ decays to determine the part involving the LCDAs from data, which is possible if all power corrections, and perturbative corrections of order $\alpha_s(m_b)$, are neglected. For the ratio (14) they find $1.27^{+0.22}_{-0.29}\,\mathrm{GeV}^2$, where we display only experimental errors. The semileptonic data provides important information on otherwise poorly constrained hadronic parameters entering these processes.

As a second example, the parameter δ measuring the relative size of hard-scattering and soft-overlap contributions in the $B \to \pi$ form factor can be related to the slope of the form factor at $q^2 = 0$ [12]. Extrapolated to zero recoil, the lattice calculations in [5, 6] give for the slope of the F_0 form factor, $\beta \equiv [(m_B^2 - m_\pi)^2 F_0'(0)/F_+(0)]^{-1} = 1.2 \pm 0.1$. Together with (13) this yields

$$\delta \equiv 1 - \frac{m_B^2 - m_\pi^2}{F_+(0)} \left(\frac{dF_+}{dq^2}\bigg|_{q^2=0} - \frac{dF_0}{dq^2}\bigg|_{q^2=0} \right) = 0.4 \pm 0.6 \pm 0.1 \pm 0.4 \,, \tag{15}$$

where the first error is experimental, the second is theoretical from the lattice determination of β, and the third is due to the form factor shape uncertainty in (13). Establishing the relative size of the hard-scattering and soft-overlap contributions from the semileptonic data provides another important input to factorization analyses of hadronic B decays. The above result for δ does not unambiguously establish $\delta \neq 0$ which signals the presence of hard-scattering terms, but it disfavors the opposite scenario, $\delta \approx 2$, where the form factor is completely dominated by hard-scattering. More data will help reduce both the experimental and shape-uncertainty errors for this quantity.

As a third example, the form factor $F_+(0)$ and shape observable α determine the coupling constant $g_{B^*B\pi}$ via

$$\frac{f_{B^*} g_{B^*B\pi}}{2m_{B^*}} \equiv \frac{F_+(0)}{1-\alpha} = 2.0\,^{+0.6}_{-1.6} \pm 0.2 \pm 1.7 \,, \tag{16}$$

where the first error is experimental, the second is theoretical from the lattice form factor normalization, and the final error is due to the form factor shape uncertainty, determined as in (13). Since the semileptonic data is concentrated at small q^2, it is not very sensitive to the detailed structure of the sub-threshold pole and dispersive integral in (1). In fact, the data do not yet definitively resolve a distinct contribution of the B^* pole, although the opposite scenario — dominance by the B^* pole in (1) — is ruled out [12].

Our implementation of the bounds in (8) and (9) could be formalized in terms of standard methods of constrained curved fitting [22]. In this language, we have enforced a "prior" probability function which is constant if the parameters obey the bound on $\sum_k |\rho_k|$ or $\sum_k a_k^2$, and zero otherwise. For simplicity, we then performed a χ^2 fit, assuming sufficient statistics that the data is Gaussian distributed. The resulting error estimates should be conservative. Firstly, this prior allows equal probability for parameter values which are near the bound, even though we expect that such values become increasingly unlikely. Other prior functions may be considered — for example, in the case of the series parameterization (5), a Gaussian prior on the variable $(-\log_{10} \sum_k a_k^2)$, with mean and standard deviation of order unity. Secondly, in estimating errors based on $\Delta\chi^2$, we neglect the fact that bounds enforce restrictions that renormalize the probability distributions, and to the extent that the bounds are relevant, this tends to overestimate errors. As a simple example, if an absolute bound happened to coincide with the boundary of the "1σ" interval obtained for an observable based on $\Delta\chi^2 = 1$, we would estimate that the observable was within the interval with only $\sim 68\%$ confidence, whereas the bounds guarantee this with 100% confidence. In a more refined analysis, a direct evaluation of the statistical integrals could account for such boundary effects. An alternative procedure employed in [9], and generalized in [23] to include shape information from experiment, has a slightly more complicated statistical interpretation. Here theory information on the form factor, combined with the dispersive bounds, is used to generate a statistical sample of "envelopes", each consisting of the curves defined at each q^2-point by the minimum and maximum values that the form factor can take. (Note that some curves may be ruled out by the bounds, yet allowed by the envelopes, which are generated by extremizing point-by-point in q^2.) This sample of envelopes is then combined with experimental branching fractions to determine a distribution for $|V_{ub}|$ or other observables. Working in terms of parameters a_k allows the experimental and lattice data to be treated on the same footing, and yields a more straightforward interpretation of the constraints enforced by the bounds.

Fortunately, these complications play an extremely minor role in the case of $|V_{ub}|$. As illustrated by Figure 1, the errors are very nearly Gaussian, and nearly identical results are obtained using different parameterizations, and widely different values for the bounds. A more refined statistical analysis might be useful for those shape observables that show sensitivity to the bounds, to extract as much information as possible from the experimental data. The methodology employed here for $|V_{ub}|$ and other parameters in semileptonic B decays can be validated in the analogous situation of semileptonic D decays, where experiment and lattice cover the entire range of q^2. We only used lattice input for the form factor at a single q^2-value, to emphasize the conclusion that the shape is determined by experiment; however, studying the form-factor shape provides an important test of lattice calculations. Our results show that with improved lattice data, an exclusive measurement of $|V_{ub}|$ that rivals or even surpasses the inclusive determination is possible.

Acknowledgments

We thank A. Kronfeld, H. Quinn and I. Stewart for discussions. We are grateful to the Institute for Nuclear Theory (Seattle, WA) for hospitality where a part of this work was completed. Research supported by the Department of Energy under Grants DE-AC02-76SF00515 and DE-AC02-76CH03000. Fermilab is operated by Universities Research Association Inc., under contract with the U.S. Department of Energy.

References

[1] S. B. Athar *et al.* [CLEO Collaboration], Phys. Rev. D **68**, 072003 (2003) [hep-ex/0304019].

[2] K. Abe *et al.* [BELLE Collaboration], hep-ex/0408145.

[3] B. Aubert [BABAR Collaboration], hep-ex/0507003.

[4] B. Aubert [BABAR Collaboration], hep-ex/0506064.

[5] M. Okamoto *et al.*, Nucl. Phys. Proc. Suppl. **140**, 461 (2005) [hep-lat/0409116].

[6] J. Shigemitsu *et al.*, hep-lat/0408019.

[7] C. Bourrely, B. Machet and E. de Rafael, Nucl. Phys. B **189**, 157 (1981).

[8] C. G. Boyd, B. Grinstein and R. F. Lebed, Phys. Rev. Lett. **74**, 4603 (1995) [hep-ph/9412324].

[9] L. Lellouch, Nucl. Phys. B **479**, 353 (1996) [hep-ph/9509358].

[10] C. G. Boyd and M. J. Savage, Phys. Rev. D **56**, 303 (1997) [hep-ph/9702300].

[11] D. Becirevic and A. B. Kaidalov, Phys. Lett. B **478**, 417 (2000) [hep-ph/9904490].

[12] R. J. Hill, hep-ph/0505129.

[13] M. C. Arnesen, B. Grinstein, I. Z. Rothstein and I. W. Stewart, Phys. Rev. Lett. **95**, 071802 (2005) [hep-ph/0504209].

[14] C. G. Boyd, B. Grinstein and R. F. Lebed, Nucl. Phys. B **461**, 493 (1996) [hep-ph/9508211].

[15] I. Caprini, L. Lellouch and M. Neubert, Nucl. Phys. B **530**, 153 (1998) [hep-ph/9712417].

[16] P. Ball and R. Zwicky, hep-ph/0507076.

[17] HFAG, http://www.slac.stanford.edu/xorg/hfag/, using

B. Aubert *et al.* [BABAR Collaboration], Phys. Rev. Lett. **94**, 181802 (2005) [hep-ex/0412037],

Y. Chao *et al.* [Belle Collaboration], Phys. Rev. D **69**, 111102 (2004) [hep-ex/0311061],

A. Bornheim *et al.* [CLEO Collaboration], Phys. Rev. D **68**, 052002 (2003) [hep-ex/0302026].

[18] J. D. Bjorken, Nucl. Phys. Proc. Suppl. **11**, 325 (1989).

[19] G. Buchalla, A. J. Buras and M. E. Lautenbacher, Rev. Mod. Phys. **68**, 1125 (1996) [hep-ph/9512380].

[20] M. Beneke and M. Neubert, Nucl. Phys. B **675**, 333 (2003) [hep-ph/0308039].

[21] C. W. Bauer, D. Pirjol, I. Z. Rothstein and I. W. Stewart, Phys. Rev. D **70**, 054015 (2004) [hep-ph/0401188].

[22] For an introduction, see G. P. Lepage, B. Clark, C. T. H. Davies, K. Hornbostel, P. B. Mackenzie, C. Morningstar and H. Trottier, Nucl. Phys. Proc. Suppl. **106**, 12 (2002) [hep-lat/0110175].

[23] M. Fukunaga and T. Onogi, Phys. Rev. D **71**, 034506 (2005) [hep-lat/0408037].